CrystEngComm

Accepted Manuscript

ROYAL SOCIETY OF CHEMISTRY

www.rsc.org/crystengcomm

CrystEngComm

Paper

Halogenated tennimides and trezimides: Impact of halogen bonding and solvent role on porous network formation and inclusion.

Received 00th October 2015,
Accepted 00th January 20xx

DOI: 10.1039/x0xx00000x

www.rsc.org/

P. Mocilac[a] and J. F. Gallagher[a*]

Fluorine and chlorine derived macrocycles (**FIO**)$_{3/4}$ and (**ClIO**)$_{3/4}$ are synthesised from the reaction of isophthaloyl dichloride with 2-amino-5-fluoropyridine and 2-amino-5-chloropyridine, respectively. Solvents of crystallisation are present in the six F/Cl crystal structures and occupy 12–43% of crystal lattice. Halogenated solvents (CH_2Cl_2; $CHCl_3$) typically link macrocycles through halogen and hydrogen bonding interactions forming 1–D chains through halogen bonding, whereas dimethylsulfoxide (DMSO) incorporation promotes solvent channel formation. For (**ClIO**)$_3$, the total (%) solvent comprising DMSO and water molecules is 43% of the structure volume with 3.5(DMSO)•3(H_2O) per (**ClIO**)$_3$ macrocycle resulting in extensive channel formation. The solvent channel aggregation assists 2–D network formation in combination with short C–Cl…O=C halogen bonding interactions and C–Cl…Cl–C contacts (Cl…O, Cl…Cl; both N_c = 0.90). Of further note is that (**ClIO**)$_4$•CH_2Cl_2 is isomorphous with two methylated analogues (**MIO**)$_4$•CH_2Cl_2 and (**MIO**)$_4$•$CHCl_3$.

Introduction

Halogen bonding research studies have evolved in the past few decades to encompass most areas of scientific research from chemistry and materials, to biology.[1] A fundamental scientific research challenge is to utilise the halogen components (usually incorporated as M–X/C–X; X = halogen) in the design and synthesis of new inorganic, organic and biological materials.[1,2] There is a key desire to exploit their unique functionality where possible, and often in a complementary role, to augment the primary role of the material.[2]

Macrocyclic science continues to develop with a multitude of studies that bridge our understanding of areas such as assembly and dynamic processes in natural and synthetic materials.[3,4] The quest towards the ideal macrocyclic platform, with the ability to fine-tune a range of physicochemical properties by simple functionalisation, currently remains a key priority in molecular recognition science and drug discovery.[4] Of major importance is the generation and investigation of new and easily accessible macrocyclic scaffolds with potential in a range of scientific fields and applications.[3,4]

We have previously reported a series of imide-based trezimide and tennimide macrocycles[5] [(**XIO**)$_{3/4}$; **X** = H, CO_2Et] and detailed the physicochemical and solid-state properties of some brominated macrocycles[5c] (**X** = Br; as in Scheme 1) where the role of the bromine atom was examined in terms of its effect in promoting 1-D supramolecular aggregation and in combination with halogenated solvents. Such macrocycles (of inherent interest in themselves for their ion-binding, selectivity, sequesterisation roles)[3-5] are important from a supramolecular perspective as possible conduits for reversible host:complex formation of, for example, waste organic/inorganic materials.[2a] Often, because of the pre-eminent role of brominated macrocycles in coupling reactions, halogenated macrocycles have been hitherto regarded as 'starting materials' *enroute* to later stage (2nd/3rd...) generation macrocyclic derivatives and largely ignored in terms of their own potentially unique properties and applications.[3,5c]

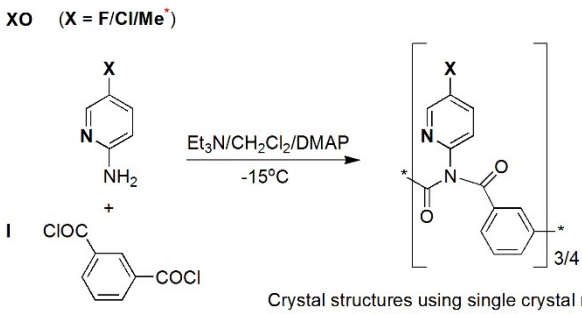

Crystal structures using single crystal methods:
(**FIO**)$_3$ as (i) CH_2Cl_2, (ii) DMSO solvate.
(**FIO**)$_4$ as (iii) $CHCl_3$, (iv) acetone solvates.
(**ClIO**)$_3$ as (v) DMSO/H_2O solvate.
(**ClIO**)$_4$ as (vi) CH_2Cl_2 solvate.
(**MIO**)$_4$* as (vii) CH_2Cl_2, (viii) $CHCl_3$ solvates.

Scheme 1 Synthesis of the (**XIO**)$_{3/4}$ (**X** = F, Cl) trezimides and tennimides. For **X** = Me*, only the tennimide (**XIO**)$_4$ was isolated and characterised.

[a] *School of Chemical Sciences, Dublin City University, Dublin 9, Ireland*.
† E-mail: john.gallagher@dcu.ie On sabbatical leave at CRM[2], Faculté des Sciences et Technologies, Université de Lorraine, BP 70239, Boulevard des Aiguelettes, 54506 Vandoeuvre-dès-Nancy, France.
Electronic Supplementary Information (ESI) available: [The ^1H, ^{13}C NMR, high resolution MS and IR spectroscopic and single crystal data for all eight macrocycles are provided with CCDC reference codes 1062025 to 1062032, together with two additional deposited CIFs as (**ClIO**)$_4$ solvents, CCDC reference codes 1062204 and 1062205]. See DOI: 10.1039/x0xx00000x

Herein, four halogenated imide-based macrocycles (**XIO**)$_{3/4}$ (**X** = **F**, **Cl**) are examined as six crystal structures and reported together with two methyl (**XIO**)$_4$ analogues, (**X** = **M** for methyl; Scheme 1). The roles that the solvent molecules play in crystal structure formation are examined and solvent volume occupied, especially where unusual synthons are observed. The impact of halogen atoms (**X** = **F**, **Cl**) in promoting 1-D chain formation and the role of solvent molecules (in an auxiliary fashion) in promoting 2-D network formation with halogen bonding is discussed. The substantial difference between the roles that halogenated solvents *e.g*. CH_2Cl_2 (dichloromethane) and $CHCl_3$ (chloroform) have in crystal structure formation is noted as compared to aprotic solvents *e.g*. DMSO (dimethylsulfoxide). In crystal structure formation, the solvent role extends beyond mere *void occupancy* to moderate halogen and hydrogen bonding interactions between the host macrocycle and halogenated solvent.[1-3]

Experimental

Materials, equipment and spectroscopic data

All chemicals, materials, vendors, spectroscopic and crystallographic as well as computational equipment are as described in the ESI and previous publications.[5] The NMR spectra experiments were performed in DMSO-d_6, at 600 MHz using a Bruker Avance Ultrashield 600 NMR Spectrometer. For the (**FIO**)$_{3/4}$ and (**ClIO**)$_{3/4}$ macrocycles, variable temperature ^{1}H-NMR, as well as ^{1}H-NMR, ^{13}C-NMR, DEPT, DEPT-Q, HSQC, HMBC, COSY and NOESY experiments were undertaken at higher temperatures (usually at 80°C). The ^{19}F-NMR experiments were undertaken on a 400 MHz Bruker NMR spectrometer for (**FIO**)$_{3/4}$ (Fig. 1). High resolution mass spectrometric data were acquired for the (**XIO**)$_{3/4}$ macrocycles and included in the Electronic Supplementary Information (ESI).

Synthesis of the (FIO)$_{3/4}$, (ClIO)$_{3/4}$ and (MIO)$_4$ macrocycles

Full synthetic procedures are provided in the ESI (Section 1). The compounds were synthesised in one step in modest yields and as reported after rigorous purification by column chromatography and recrystallisations. The (**MIO**)$_3$ derivative was not isolated from the reaction although there was an indication that it forms in very low yield (<1–2%) but proved elusive in order to separate, isolate and characterise. This may be due to a preferred conformation in a precursor with a favourable conformation towards tetramer and/or oligomer formation.

The (**FIO**)$_{3/4}$ synthesis is as described for the '4+4' condensation reaction[6] using 2-amino-5-fluoropyridine (1.0986 g, 9.8 mmol) as a functionalised 2-aminopyridine. The polymeric product did not precipitate and the reaction mixture stayed clear overnight, suggesting improved polymer solubility. Chromatographic purification and separation used a mobile phase containing $CHCl_3$ and ethyl acetate (4:1), yielding the (**FIO**)$_4$ tennimide (140 mg, 5.9%, R_f = 0.3) and (**FIO**)$_3$ trezimide (150 mg, 6.3%, R_f = 0.2). The isolated (**FIO**)$_3$ had minor amounts of the tetramer (**FIO**)$_4$ and final purification was accomplished using preparative TLC plates. The (**FIO**)$_{3/4}$ macrocycles have similar white colours and properties to the parent (**IO**)$_{3/4}$ macrocycles,[5a] but with better solubility, especially in chlorinated hydrocarbon solvents.

Synthesis of the (**ClIO**)$_{3/4}$ macrocycles (as described for (**FIO**)$_{3/4}$) used 2-amino-5-chloropyridine (1.2599 g, 9.8 mmol) as the functionalised 2-aminopyridine. The major difference is that a polymeric product precipitates and is removed by filtration, as for the (**IO**)$_{3/4}$, (**26IO**)$_{3/4}$ macrocycles and brominated analogues.[5a,c] Column chromatography (similar to the (**FIO**)$_{3/4}$ purification) yields (**ClIO**)$_4$ (197 mg, 7.7%, R_f = 0.60) and (**ClIO**)$_3$ (120 mg, 4.7%, R_f = 0.39). The (**ClIO**)$_{3/4}$ macrocycles have similar properties to the analogous fluoro derivatives; white, odourless crystalline solids with a yellow tinge although their solubility is slightly less than their fluoro analogues in organic solvents.

The (**MIO**)$_4$ tennimide was synthesised using 2-amino-5-methylpyridine (6-amino-3-picolinate, 1.0600 g, 9.8 mmol). The crude product was purified by column chromatography eluting using a solvent blend of $CHCl_3$ and ethyl acetate (2:1). Although an additional compound was detected by TLC and possibly as the (**MIO**)$_3$ trezimide, only separation of the first fraction was successful as (**MIO**)$_4$, (110 mg, 5%, R_f = 0.27). The (**MIO**)$_4$ tennimide is a white, moderately crystalline solid, readily soluble in $CHCl_3$, CH_2Cl_2, ethyl acetate and MeOH, but less soluble in diethyl ether and insoluble in water or *n*-hexane.

Single-crystal growth and X-ray crystallography methods

All crystal samples were obtained by slow evaporation at room temperature or 4°C, typically from CH_2Cl_2, $CHCl_3$ ($CDCl_3$), $(CH_3)_2CO$ acetone and DMSO. Single crystal growth was successful for all macrocycles from the original solvent or from solvent combinations. Single crystal X-ray data collection, data reduction,[7] structure solution and refinement[8] for all eight crystal structures (to final conventional R = 3.5 to 6.4%) are as reported.[5] Selected crystallographic and structural information are provided in the ESI (Section 5) with hydrogen bonding details (Table 1). Molecular and packing diagrams (Figs 2-6) were generated using ORTEP (with displacement ellipsoids at the 10-30% probability level) and MercuryCSD.[9] The Cambridge Structural Database was analysed using the 2015 version.[10] For (**ClIO**)$_3$, the SQUEEZE program in PLATON[9a] was used to eliminate regions of diffuse electron density in solvent accessible sites (additional details available).

Crystal structures, solvates (void analysis) and refinement issues

All crystal samples crystallised with disordered solvent molecules and several strategies were employed to handle the disorder. The eight crystal structures include the three (**FIO**)$_3$•CH_2Cl_2, (**FIO**)$_3$•DMSO and (**ClIO**)$_3$•(3.5DMSO:3H_2O) trezimides and five (**FIO**)$_4$•$CHCl_3$, (**FIO**)$_4$•2(acetone), (**ClIO**)$_4$•CH_2Cl_2, (**MIO**)$_4$•CH_2Cl_2 and (**MIO**)$_4$•$CHCl_3$ tennimides, (trezimide/tennimide designator is used in preference to numerals).[5] In addition, crystal structures of (**ClIO**)$_4$•0.8$CHCl_3$ and (**ClIO**)$_4$•0.61CH_2Cl_2 (second CH_2Cl_2 solvate; weak diffractor) have been determined but are not discussed herein for brevity (salient details in ESI). Comparisons are made with solvent structures reported by Yufit and Howard.[11]

In the (**FIO**)$_3$•CH_2Cl_2 structure (apart from disordered CH_2Cl_2 with 0.904(6):0.096(6) sites and treated with modest restraints), refinement proceeded without problem. Likewise in (**FIO**)$_3$•DMSO, the disordered DMSO molecule (as 0.775:0.225) was treated for disorder without refinement or convergence problems and both

structures have solvent molecules that occupy a total of 16% of their respective unit cell volumes.

In the (**ClIO**)$_3$•(DMSO/H_2O) structure, solvent problems manifested in the latter stages of refinement where the nature of the solvent composition and disorder was elucidated to total 3.5 disordered DMSO sites and 3 water molecules (disordered with partial occupancy over several sites) per asymmetric unit. Analysis indicated that 43% of the unit cell contained solvent.[9a] Refinement to *R* = 7% was unsatisfactory (with trezimide included and appropriate modelling of the solvent site occupancy with disorder). Therefore, the majority of partial occupancy water molecules/sites were eliminated and only 'well-behaved' though disordered DMSO molecules and two water sites were retained in refinement prior to application of SQUEEZE[9a]; refinement then converged to *R* = 5%.[8] Solvent molecules not included in refinement are located in 8 channels per unit cell (4 within; 8 shared) aligning along the *c*-axis in space group *Fdd2*. The total solvent molecule occupancy (as DMSO/H_2O) accounts for 9220 Å^3 (43%) of the crystal structure with this solvent volume allocated as 26% (refined atom sites) and 17% solvent volume with estimated electron density from SQUEEZE.[9a] The final DMSO site occupancy factors are 0.75:0.25 (general positions), 0.40 (2–fold axes), 0.48 (with two partial occupancy water sites). For each (**ClIO**)$_3$ macrocycle there are 3.5 DMSO and 3 water molecules. Therefore, the solvent occupancy sites per (**ClIO**)$_3$ are calculated as 3.5 × (130 Å^3) (as 3.5 DMSO solvent molecules) plus 120 Å^3 (for 3 H_2O molecules) = 575 Å^3 per asymmetric unit.

In (**FIO**)$_4$•$CHCl_3$, disordered $CHCl_3$ (as 77:23 site occupancy; 14% of the unit cell) presented no problems in refinement. There is no evidence of disorder in the pyridinyl ring from bond length analysis and difference maps of the residual electron density, although disordered ring components with site occupancy factors < 20% would barely be detectable when superimposed after rotation of the *ortho*-pyridine ring by 180°. Refinement was undertaken with four pyridinyl rings at 100% site occupancy (in one orientation only).[8] In (**FIO**)$_4$•2(acetone), the (**FIO**)$_4$ crystallises with two acetone molecules in the asymmetric unit (20% of the volume), one is 50:50 disordered over two sites, whereas the ordered acetone has large displacement parameters, but refines satisfactorily using appropriate DFIX restraints on bonds and angles.

For (**ClIO**)$_4$, analysis of the pendant pyridine rings in (**ClIO**)$_4$•(CH_2Cl_2) from bond length analysis and difference maps indicates that the N12A and N22A pyridine rings are disordered. This is not surprising given that the pyridine rings in the related (**BrIO**)$_4$ are disordered,[5c] but such that it is barely discernible, apart from less clearly defined pyridine ring bond lengths and slightly larger displacement ellipsoids (the (**IO**)$_4$ and related (**FIO**)$_4$ structures do not exhibit any disorder in their scaffolds). Refinement of (**ClIO**)$_4$ was initially performed with pyridine rings as rigid hexagons but without satisfactory convergence; subsequently moderate DFIX/FLAT restraints were applied to the C11A/C11B pyridine rings with appropriate pyridine C–C/C–N bond length restraints.[8] The Cl14 and Cl24 chlorines have large displacement parameters but there is no indication of splitting and both of the pyridine ring Cl components effectively occupy the same site (disorder from 180° rotation about the Cl–C_{para}…C_{ipso} axis). For the (**ClIO**)$_4$•(CH_2Cl_2) structure, solvent disorder is noted as a full occupancy CH_2Cl_2 molecule disordered about a 2–fold axis with large displacement parameters.

The (**MIO**)$_4$ structures (CH_2Cl_2; $CHCl_3$ solvates) crystallise in *Pccn* with both solvent molecules occupying 12% unit cell and are isomorphous/isostructural with (**ClIO**)$_4$•CH_2Cl_2 and (**BrIO**)$_4$•$CHCl_3$.[5c] For the CH_2Cl_2 structure, pyridine ring disorder was treated using DFIX/FLAT commands and one methyl group (C27) given site occupancies of 0.5:0.5 (as atom sites were split due to the ring disorder). The CH_2Cl_2 molecule is disordered at 0.5:0.5 site occupancy about a 2–fold axis. The $CHCl_3$ solvate had minor refinement issues but is similar to (**MIO**)$_4$•CH_2Cl_2. In addition the (**ClIO**)$_4$ structures (**ClIO**)$_4$•0.8($CHCl_3$) and (**ClIO**)$_4$•0.61(CH_2Cl_2) (details in the ESI) are isomorphous with (**ClIO**)$_4$•(CH_2Cl_2) and (**MIO**)$_4$ methylated analogues. They exhibit similar refinement problems and disordered halogen bonding between the macrocycle and solvent molecules.[12]

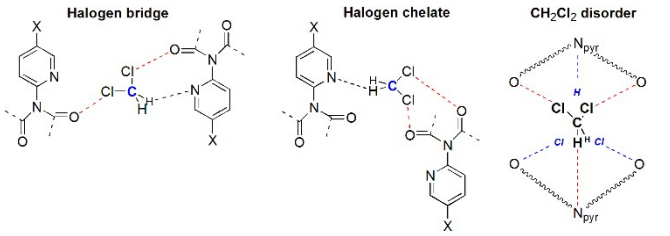

Scheme 2 Depiction of CH_2Cl_2 (or $CHCl_3$) interacting with macrocycles *via* hydrogen and halogen bonding (bridging/chelating modes). Interactions are swopped between chelating on either side or bridging/linking the macrocycles by disorder.

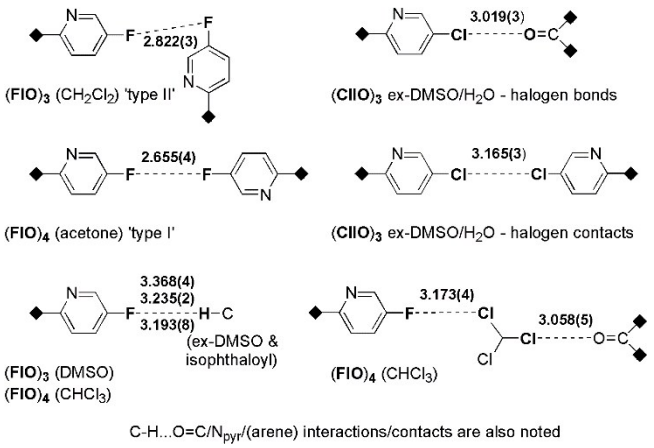

Scheme 3 Primary halogen and hydrogen bonding interactions and contacts (distances, Å).

Results and discussion

Comments on the spectroscopic data

Spectroscopic data are provided in the ESI as ^{1}H-, ^{13}C-NMR (Section 2), IR (Section 3) and MS/HRMS data (Section 4). The NMR data, recorded in both $CDCl_3$ (^{1}H-NMR) and DMSO (^{1}H-, ^{13}C-, ^{19}F NMR), are as expected and include variable temperature (VT) studies. Preparative TLC plates were purchased from Analtech Inc., USA.

NMR experiments for the (**FIO**)$_{3/4}$ macrocycles were performed initially at room temperature (293 K) and 353 K (^{1}H, ^{13}C, ^{19}F-NMR data in ESI; Fig. 1) and are comparable with the original (**IO**)$_{3/4}$

systems[5a] (^{19}F-NMR experiments included VT studies). In **(FIO)$_3$** at 293 K, two rather weak and broad signals are observed at -129.8 and -128.7 ppm. These signals merge and coalesce into one signal (on increasing the temperature to 313 K) that intensifies and sharpens at -129.2 ppm on increasing the temperature to 353 K (80°C). In **(FIO)$_4$** at 293 K, two broad and weak signals (but more clearly resolved than for **(FIO)$_3$**) are positioned at -127.5 and -128.5 ppm that coalesce on increasing the temperature to 313 K, and intensifying at -128.1 ppm (on raising the temperature to 353 K). The VT-NMR results suggest the existence of two conformers in both **(FIO)$_{3/4}$** macrocycles at room temperature and with relatively low energy differences between each of the conformer pairs. This has been noted previously with two distinct **P** and **R** conformations observed structurally for the trezimides (with **P** as the more common).[5a] The **(FIO)$_4$** NMR data indicate the presence of a 2nd distinct conformation that has remained elusive to date and is different to the known (*syn*)$_4$ conformation[5] and is possibly a combination of *e.g*. (*syn*/*anti*)$_2$ or (*syn*)$_3$/(*anti*) or (*syn*)/(*anti*)$_3$ conformations that interconvert to a more stable averaged conformation on heating in solution.[5] Presumably, interconversion between conformations leads to an averaged structure in DMSO-d_6 solution on warming to 310-320 K.

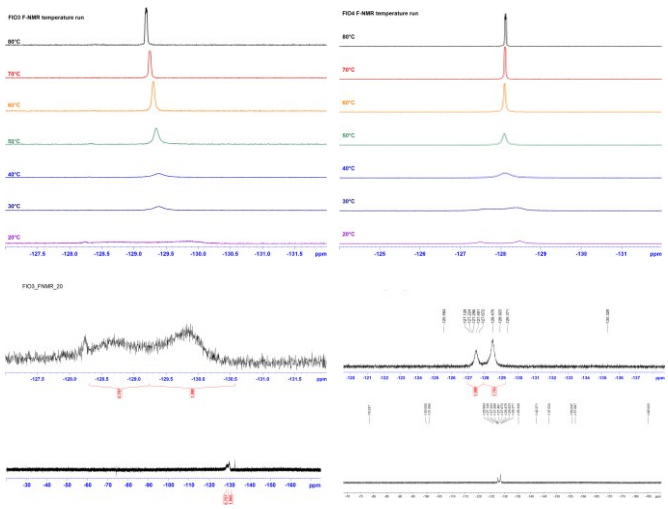

Fig. 1: ^{19}F NMR for **(FIO)$_3$** at 20°C (left) and VT studies to 80°C (top); **(FIO)$_4$** at 20°C (right) and VT studies to 80°C (top).

The infra-red data for **(FIO)$_3$** reveal additional peaks in the 2800-3100 cm^{-1} region suggesting that the bulk **(FIO)$_3$** crystalline material is in the form of a solvate. The NMR and IR data for the **(ClIO)$_{3/4}$** macrocycles (^{1}H-,^{13}C-NMR data at 80°C in the ESI) are very similar to the **(FIO)$_{3/4}$** results and will not be discussed further. The ^{1}H-NMR experiments for **(MIO)$_4$** in DMSO-d_6 at 80°C show good resolution of the macrocyclic tennimide core proton peaks with the methyl peak observed at 2 ppm, while the ^{13}C-NMR (under the same conditions) has the methyl carbon at 17.25 ppm. No evidence of instability was detected by NMR experiments suggesting that the overall macrocyclic stability of the **(MIO)$_4$**, **(FIO)$_4$** and **(ClIO)$_4$** tennimides are comparable with their parent **(IO)$_4$** tennimide.[5a]

Comments on the molecular structures

The eight **(FIO)$_{3/4}$**, **(ClIO)$_{3/4}$** and **(MIO)$_4$** crystal structure details are discussed and are listed in Sections 5.1-5.3 (of the ESI). The salient features of hydrogen bonding are as listed in Table 1 and halogen bonding details in Scheme 3 (ESI).[8] Comparisons can be made with the molecular structures of the related trezimides[5] and tennimides.[5,6] For the trezimides which have asymmetric structures and adopting the **P** conformation,[5] the isophthaloyl O…O, imide O…O and N…N distances typically lie within the expected values with the **(FIO)$_3$**•DMSO structure displaying the greatest variations from average values. For all three trezimides the imide N atom exhibits pyramidal behaviour as expected with the N atom in a range from 0.101(2) to 0.226(2) Å (from the three C atom plane to which N is bonded). The isophthaloyl and imide O=C…C=O define the conformation of the primary groups and show broad similarities in conformation with two *syn*-torsion angles for the isophthaloyl and one oriented differently, whereas for the imide OCCO torsion angles these are usually oriented in orthogonal directions in a range from *ca*. 90 to 105° (ESI: Section 5.3). These are typical values for the **P** conformation, as noted in all but one of the trezimide conformations reported.[5]

In the five tennimides comprising two **(FIO)$_4$**, **(ClIO)$_4$** and two **(MIO)$_4$** crystal structures the conformations are all (*syn*)$_4$ with respect to the isophthaloyl O=C…C=O torsion angles. The symmetrical nature of the tennimides is shown in **(FIO)$_4$**•(acetone)$_2$ where the four fluorine atoms exhibit a reasonably symmetrical tetrahedral disposition as defined by the six F…F separations in a range from 10.091(5) to 10.566(4) Å and with six imide N…N distances from 5.238(2) to 5.939(2) Å. For the **(ClIO)$_4$** structure with 2-fold symmetry the Cl…Cl distances are from 10.7944(15) to 11.359(2) Å demonstrating the tetrahedral arrangement of the Cl atoms (with imide N…N from 5.195(3) to 5.867(4) Å). The crystal and molecular structures will be discussed in the following section.

Comparisons of the solid state structures

Three (FIO)$_3$ and (ClIO)$_3$ crystal structures

Assembly usually involves solvent molecules occupying the macrocyclic niches and pockets with aggregation usually as 1-D chains. The **(FIO)$_3$** macrocycle crystallises as CH_2Cl_2 and DMSO solvent molecules with **(FIO)$_3$**•CH_2Cl_2 having the CH_2Cl_2 partially residing in a molecular niche of the asymmetric **(FIO)$_3$** conformation as defined by the two fluoropyridine rings and an isophthaloyl group. Two symmetry related CH_2Cl_2 solvent molecules comprise a 'solvent pocket' as enveloped by six **(FIO)$_3$** trezimides; the various modes of halogen bonding interactions of solvent with the macrocycles are depicted in Schemes 2 and 3.

D—H···*A*	*D*—H	H···*A*	*D*···*A*	*D*—H···*A*
(FIO)$_3$•CH_2Cl_2				
C34—H34···O2^{i}	0.93	2.52	2.976(2)	110
C35—H35···O1^{ii}	0.93	2.37	3.135(2)	139
C12—H12···N3	0.93	2.61	2.917(2)	100
C22—H22···N1	0.93	2.60	2.911(2)	100
(FIO)$_3$•DMSO				
C2S—H2S3···F24A^{iii}	0.96	2.52	3.368(4)	148
C15—H15···F14A^{iv}	0.93	2.54	3.235(2)	132
C23A—H23A···O6^{ii}	0.93	2.45	3.316(3)	155

C34—H34···N12A^{iii}	0.93	2.51	3.364(2)	152
(**FIO**)$_4$•CHCl$_3$				
C1A—H1A···F34A^{v}	0.98	2.37	3.193(8)	141
C15—H15···O6^{vi}	0.93	2.56	3.456(4)	162
C42—H42···N4	0.93	2.57	2.897(4)	101
C45—H45···O4^{ii}	0.93	2.57	3.273(4)	133
C45A—H45A···O7^{vii}	0.93	2.51	3.270(5)	139
(**FIO**)$_4$•(acetone)$_2$				
C2B—H2B2···O4^{viii}	0.96	2.54	3.091(10)	117
C15—H15···O4^{ix}	0.93	2.58	3.475(5)	161
C15A—H15A···O1A^{viii}	0.93	2.32	3.240(10)	168
C24—H24···O1B^{ii}	0.93	2.44	3.189(12)	138
C25A—H25A···O2A^{x}	0.93	2.43	3.349(12)	170
C26A—H26A···F34A^{ii}	0.93	2.51	3.383(5)	156
C33A—H33A···O2A^{xi}	0.93	2.53	3.377(11)	152
(**ClIO**)$_4$•CH$_2$Cl$_2$				
C13B—H13B···O4^{xii}	0.93	2.48	3.365(15)	158
C12—H12···N1	0.93	2.58	2.902(3)	101
(**MIO**)$_4$•CH$_2$Cl$_2$				
C12—H12···N1	0.93	2.58	2.898(4)	100
(**MIO**)$_4$•CHCl$_3$				
C22—H22···N2	0.93	2.59	2.910(3)	100
C23A—H23A···O2^{xiii}	0.93	2.48	3.251(14)	141

Symmetry codes: (i) *-x*, *y*+1/2, *-z*+1/2; (ii) *x*-1, *y*, *z*; (iii) *x*+1/2, *-y*+1/2, *z*-1/2; (iv) *-x*+3/2, *y*+1/2, *-z*+1/2; (v) *x*, *y*+1, *z*; (vi) *x*, *y*-1, *z*; (vii) *-x*+1, *-y*, *-z*+1; (viii) *-x*, *-y*, *-z*+1; (ix) *x*+1, *y*, *z*; (x) *-x*-1/2, *y*+1/2, *-z*+1/2; (xi) *-x*+1/2, *y*+1/2, *-z*+1/2; (xii) *-x*+2, *-y*, *-z*; (xiii) *-x*, *-y*+1, *-z*.

Table 1: Selected hydrogen bonding details (Å,°)†

The (**FIO**)$_3$ macrocyclic geometry is broadly similar to both (**IO**)$_3$[5a] and (**BrIO**)$_3$[5c] (Tables 2,3) and highlighting the semi-flexible nature of the 18-atom macrocyclic scaffold at room temperature (RT) across several derivatives (based on both NMR and structural data). This (**FIO**)$_3$ trezimide comprises two parallel fluoropyridines with *cis*-related N atoms separated by 5.646(2) Å (the *cis*-related F14A…F34A = 4.059(2) Å) and adopting the known **P** conformation.[5a] This macrocyclic conformation is distorted and with considerable twisting and bending of the isophthaloyl aromatic groups but without disorder within the scaffold backbone. The crystal structure consists of an array of non-classical weaker intra-/intermolecular C-H...N/O hydrogen bonds together with halogen…halogen (F…F) interactions. The latter include C-F…(F-C)^{i} contacts in a *T*-shaped arrangement as C24A-F24A…(F14A-C14A)^{i} (*i* = 1-x,1/2+y,1/2-z).[13] The F24A…F14A^{i} (N_c = 0.96) and F24A…C14A^{i} distances are 2.822(3) Å and 3.080(3) Å (*ca*. 0.10 Å < the van der Waals radii sum) with C24A-F24A...F14A^{i} and F24A...(F14A-C14A)^{i} angles of 146.98(15)° and 87.73(13)°, respectively. The data are similar to that reported by Wozniak and co-workers and closer to ideal type *II* values.[13] A C35-H35...O1 intermolecular interaction is noted aligning along the *a*-axis direction amidst a myriad of intermolecular contacts. Despite the plethora of potential interactions that can potentially arise, crystal structure formation usually occurs from a couple of moderately strong interactions.[1,12]

For the (**FIO**)$_3$•DMSO structure (Fig. 2), a disordered DMSO molecule resides in the macrocycle niche with the DMSO oxygen atom oriented into the cleft. The scaffold differs slightly from the CH_2Cl_2 solvent molecule as discussed (Table 2) and mainly in the orientation of the pendant pyridine ring (at F24A). The *cis*-related F atoms are separated by 3.641(2) Å [4.059(2) Å, CH_2Cl_2] and *cis*-pyridine N atoms by 5.240(2) Å [5.646(2) Å] and demonstrating the semi-flexible nature of the trezimide **P** conformations. No macrocyclic disorder is observed but there is considerable aromatic ring bending and group deformation. There are no interactions of note in (**FIO**)$_3$•DMSO apart from weak C-H...O interactions assisting in the overall packing and stacking together with several contacts *e.g*. as C4=O4...π(arene). In packing, DMSO molecules are additionally surrounded by four (**FIO**)$_3$ *via* weak intermolecular interactions.

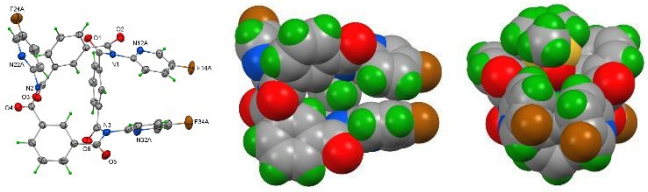

Fig. 2: An ORTEP plot of (**FIO**)$_3$ with displacement ellipsoids at the 25% level; views of the macrocyclic core (and niche) and with the DMSO solvent included with atoms as van der Waals spheres.

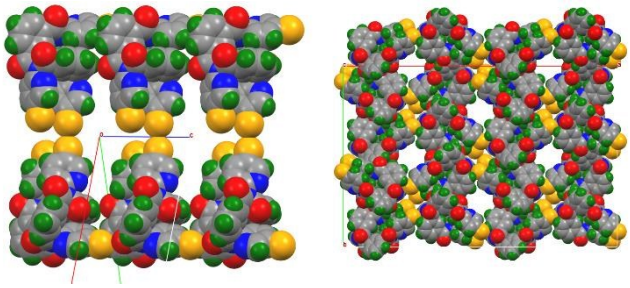

Fig. 3: A view of the (**ClIO**)$_3$ 2D structure (with Cl…O=C interactions and Cl…Cl contacts) and 3D solvent voids with atoms drawn as van der Waals spheres.

The (**ClIO**)$_3$ macrocyclic scaffold is similar to (**FIO**)$_3$, though there are several key differences in the crystal structure with (**ClIO**)$_3$ crystallising with a complex and disordered array of DMSO and water solvent molecules occupying 43% of the lattice. The (**ClIO**)$_3$ molecules are arranged such that the solvent molecules aggregate in channels through the crystal lattice. A relatively short intramolecular distance is also observed between two *cis*-related Cl14 and Cl34 atoms in *quasi*-parallel pyridine rings with Cl14…Cl34 = 3.660(3) Å (Fig. 3) and as observed for the *cis*-related pyridine N atom separation in (**FIO**)$_3$•DMSO.

>>> Table 2 to be placed here at the top of this page

Table 2: Comparisons of **(FIO)$_3$**, **(ClIO)$_3$** with **(IO)$_3$**[a] and **(BrIO)$_3$**[d]

Halogen bonding interactions, contacts[16a] *and 2D network formation in* (**ClIO**)$_3$

There is an intermolecular interaction and a significant contact involving the Cl atoms.[14-16] These are (*a*) the C24A-Cl24…(O4=C4)^{iii} halogen bond with Cl24…O4^{iii} = 3.019(3) Å (*iii* = x,y,1+z; N_c = 0.90)

and (*b*) the symmetrical Cl34…Cl34^{ii} = 3.165(3) Å halogen…halogen contact with C-Cl…Cl = 154.33(19)° in a *trans* type *I* arrangement (about a 2-fold axis in *Fdd2*; *ii* = -x,-y,z; N_c = 0.90).[13,16] The influence of both of these on crystal structure formation is interesting. As the C-Cl…Cl and Cl…Cl contact details are broadly similar to bromotrezimides (on geometric grounds; N_c ~ 0.90) this will be considered first.[5c] From CSD[10] analysis of aromatic C_6-Cl...Cl-C_6 intermolecular distances, the Cl34...Cl34^{ii} contact distance (Å) of 3.165(3) Å is within the shortest range (1-2%)[15] of ~1700 CSD entries[10] (2274 hits, R < 0.10, no errors/disorder or polymers/powders) for Cl...Cl intermolecular contact distances from 0 to 3.5 Å (mean = 3.39 Å) and C-Cl…Cl angles 120→180° (median = 152°).[14-15] For comparisons, Mondal and co-workers reported coordination polymers with $_{aromatic}$C-Cl…Cl-C halogen bonding interactions.[15] Their EBITEQ[10,15] structure has a Cl...Cl* = 3.112(1) Å (N_c = 0.89), C-Cl...Cl* = 165.6(2)° and similar geometrically to our symmetrical type *I* contact in (**ClIO**)$_3$. Their 1D coordination polymer assembles into 2D grids by short (type *I*) Cl...Cl* interactions.[15]

In (**ClIO**)$_3$ the Cl24...(O4=C4)^{iii} halogen bonding interaction forms chains along (001). Chains aggregate as a column, with a second chain (related by a 2-fold axis) *seemingly* interlocked by the short Cl34...Cl34^{ii} contacts, assisted by longer Cl...N intermolecular interactions. However, disordered DMSO and water molecules in proximity to the C-Cl34...(Cl34-C)^{ii} contacts are the primary driving force in aggregation (strong hydrogen bonding interactions involving H_2O), but this is difficult to quantify (given the extent of solvent disorder). The two-molecule wide columns weakly interact with neighbouring columns forming a 2D sheet, with inter-sheet van der Waals contacts involving (**ClIO**)$_3$. The DMSO/H_2O molecules in channels between the columns play a critical role in aggregation and crystallisation. From studies on C-Br...O=C/N halogen bonding[5c] where the driving force to form 1D halogen bonded chains at least is favourable, the utilisation of the 2-3 remaining halogen atoms has been at best unremarkable. In (**ClIO**)$_3$ the main C-Cl...O=C halogen bonding drives 1D chain formation in combination with strong hydrogen bonding (solvent) interactions in channels and helps to stabilise the crystal structure. The short C-Cl34...Cl34-C[16a] contact facilitates aggregation of two molecule wide chains into ladders (though compensated by the solvent channel). The exact nature of the short C-Cl...Cl-C contact is difficult to quantify; it is presumably weakly repulsive, with neighbouring solvent molecules (and the pyridinyl *meta*-N atom) modulating this to some degree.[16]

The question arises as to whether (**ClIO**)$_3$•(DMSO)$_{3.5}$•(H_2O)$_3$ should be regarded as (*i*) a host macrocycle crystal structure with solvent molecules filling the lattice voids (channels) or (*ii*) with the DMSO, H_2O molecules behaving as strongly interacting molecules stabilising and holding the macrocycles? The structure can be regarded as intermediate with halogen bonding and solvent channels both playing key roles in the channel and molecular superstructure. The halogen bonding distances are key starting points for geometrical analysis, but electrostatic, dispersion and polarisation effects also need to be addressed in a complex structure as (**ClIO**)$_3$.[13-14,16-17] As such the role of atom...atom interactions in crystal structures has been the subject of much discourse over several decades and recently by Dunitz,[17a] Desiraju *et al*.,[17b] and Lecomte and co-workers.[17c] The (**ClIO**)$_3$ trezimide (itself lacking strong hydrogen bond donors) allows the analysis of complex halogen bonding arrangements with several halogens capable of forming weak to moderate strength halogen bonds relative to stronger hydrogen bonding, weaker interactions and contacts.[1,12,16a] Although there are broad similarities in molecular geometry between the four macrocycles in the trezimide series (**Table 2**), both (**IO**)$_3$ and (**ClIO**)$_3$ are more closely matched (with DMSO), while (**FIO**)$_3$ and (**BrIO**)$_3$ show similarities, crystallising from the less polar CH_2Cl_2 and EtOAc, respectively.

Three (FIO)$_4$ and (ClIO)$_4$ molecular and crystal structures

(**FIO**)$_4$ was analysed as both $CHCl_3$ and $(CH_3)_2CO$ solvates. (**FIO**)$_4$•$CHCl_3$ crystallises with a disordered $CHCl_3$ and its overall geometry is similar to that of (**IO**)$_4$ and (**BrIO**)$_4$,[5a,c] (Table 3) as evidenced by the semi-flexible nature of the 24-atom macrocyclic scaffold. This tennimide has an *open-closed* arrangement at the macrocyclic cavity entrances as noted by geometric differences *e.g*. H...N and from the O...O$_{imide/isophthaloyl}$ distances (Table 3).

Short C-H...F and F...F interactions in (**FIO**)$_4$

The (**FIO**)$_4$ crystal structure comprises an array of non-classical, weak intra-/intermolecular C-H...N/O hydrogen bonds. Of note, a short C1A-H1A...F34A interaction, comprising the $CHCl_3$ molecule and a *para*-fluorine, assists in aggregation (H1A...F34A = 2.37 Å, N_c = 0.89) (Fig. 4). In addition, the $CHCl_3$ molecule partially resides in a lattice void and engaging in halogen bonding as C-F...Cl-C (F44A...Cl1A^{iv} = 3.173(4) Å, *iv* = 1-x,1-y,1-z) and C-Cl...O=C (Cl2A...O1^{v} = 3.058(5) Å, *v* = -1+x,1+y,z). The role of $CHCl_3$ in (**FIO**)$_4$ crystal structure formation is to link adjacent macrocycles by way of an unusual macrocycle:$CHCl_3$ aggregate. Whereas solvent molecules are frequently incorporated into lattices during crystallisation, the roles that halogenated solvents play in crystallisation and the stability of such crystal structures is still not well understood.[11] It is also difficult to analyse the dynamics (computational expense) from a molecular modelling viewpoint. Solvent molecules are often considered as void fillers and especially where the solvent is small in comparison with the host molecule. Yet structural information as to the solvent role can be obtained from analysis of the intermolecular geometric data in the absence of more detailed information, though one needs to proceed with caution.[17] In the (**FIO**)$_4$ macrocycles, short C=O...π(arene) contacts also form about inversion centres with O7...(ring centroid)^{iv} = 3.333(3) Å and O7...C24A^{iv} = 3.046(4) Å.

>>> Table 3 to be placed at the top of this page

Table 3: (**XIO**)$_4$ geometric data (Å) (with X = H, F, Cl, CH_3, Br)

The (**FIO**)$_4$•(Me_2CO)$_2$ structure has acetone assisting in molecular aggregation such that tennimides align as columns and partially disordered acetone solvent molecules in channels (20% of cell volume), that align in a defined direction and parallel with the (10-1) plane (Fig. 4). The (**FIO**)$_4$ crystal structure consists of an array of non-classical, weaker intra-/intermolecular C-H...N/O/F hydrogen bonds yet cumulatively important *e.g*. reciprocal C46-H46...N32A$_{pyr}$ interactions about inversion centres. There is a distinct C-F...(F-C)^{v} contact (N_c = 0.90) that is relatively linear as C24A-F24A...(F44A-C44A)^{v} with C24A-F24A...F44A^{v} and F24A...(F44A-C44A)^{v} angles of

169.1(6)°, 149.7(4)°, respectively, with F24A...F44A^{v}, F24A...C44A^{v} separations of 2.655(4) Å, 3.980(6) Å (*ca*. 0.30 Å < van der Waals radii sum).[13,16a] Analysis (CSD)[10] for C_6-F...F-C_6 intermolecular interactions/contacts demonstrates that the F24A...F44A^{v} contact distance is within the shortest 2-3% of 3209 entries (8273 hits, R < 0.10, no errors/disorder/polymers/powder structures)[10] for F...F intermolecular distances from 0→3.5 Å and C-F...F angles from 120-180° (median distance/angle = 2.85 Å/142°).[10] Finally, the C15A-H35...O1A$^{\#}$ intermolecular interaction (# = -½-x,½+y,½-z) involves an acetone molecule amidst a multitude of weaker contacts. Despite the plethora of potential interactions that can form, crystallisation occurs from moderately strong XB interactions.[1,12]

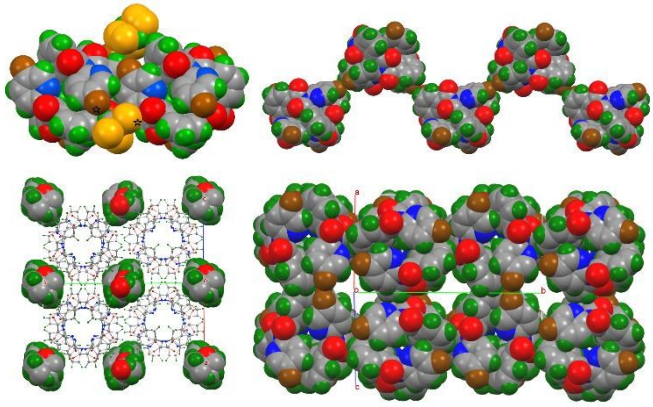

Fig. 4: Views of the C-H...F and Cl...O=C interactions (marked as ★) in (**FIO**)$_4$ $CHCl_3$ and F...F contact distance of 2.655(4) Å in (**FIO**)$_4$•2(acetone) (top); two views of the acetone channels and acetone solvent channels in (**FIO**)$_4$•2(acetone) (bottom).

(**ClIO**)$_4$ is isomorphous with the (**BrIO**)$_4$ analogue (in space group *Pccn*)[5c], but not with either of the (**IO**)$_4$ or (**FIO**)$_4$ structures; this type of isomorphous pairing in halogen derivatives is well known.[10,18] For these structures, the role of the CH_2Cl_2 or $CHCl_3$ solvent molecules is to link macrocycles. For comparisons, in the parent (**IO**)$_4$ structure,[5a] disordered $CHCl_3$ form 1:1 aggregates with the (**IO**)$_4$ macrocycle by two key C=O...Cl-C interactions and with an unusual cyclic C-Cl...O=C moiety centred on $CHCl_3$. The $CHCl_3$ molecule also forms a C-H...$N_{pyridine}$ interaction (and C-H...Cl-C interactions, 2.61 Å) and aggregates about an inversion centre to form a four macrocycle cluster with two disordered $CHCl_3$ as linkers.

An unusual solvent...imide (macrocycle) arrangement in (**ClIO**)$_4$

The CH_2Cl_2 solvent molecule occupies a pocket (12% of unit cell volume) between the macrocycles. Refinement of the disordered CH_2Cl_2 (50:50% occupancy about a 2-fold axis) and disordered pyridine rings (0.5:0.5) in (**ClIO**)$_4$ is demonstrated by the partial C-H...N hydrogen bond forming between one CH_2Cl_2 orientation and one of the pyridine conformations. The disorder reveals one CH_2Cl_2 conformation (50%) as py...H-C-Cl...O=C (two imide groups) or reversed (50%) and the C-Cl...O=C (XBs) have N_c values of 0.88, 0.91. The dichloromethane H_2CCl_2 uses its two Cl atoms to span the imide group carbonyl oxygen atoms O1/O2 and form an unusual cyclic solvent...imide aggregate [$R^2_2(8)$ ring] as (1:1) CH_2Cl_2:(**ClIO**)$_4$. Given that there is disorder present there is also the possibility of a minor component of CH_2Cl_2 spanning both macrocycles as a linker molecule (Fig. 5). Analysis demonstrates the ability of CH_2Cl_2 through disorder to link macrocycles through hydrogen (C–H…N) and halogen bonding (C–Cl…O=C interactions).[12] In assembly (**ClIO**)$_4$•CH_2Cl_2 moieties align as 1-D chains along the *a*-axis. The replacement of solvent linkers on replacement of CH_2Cl_2 by $CHCl_3$ (ESI) leads to an increase in the unit cell parameter [volume] from 13.8337(1) Å [5018.11(5) Å^3] to 13.9915(6) Å [5095.2(4) Å^3] with only minor changes in the halogenated solvent environment. A second CH_2Cl_2 structure as (**ClIO**)$_4$•0.61CH_2Cl_2 shows the retention of the crystal structure in space group *Pccn* even when only partial occupancy solvent is present and contraction of the unit cell *a* length to 13.6868 (9) Å, [4974.0(5) Å^3] (ESI).

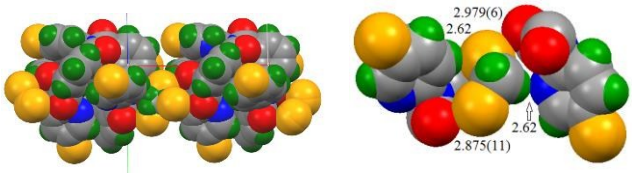

Fig. 5: Views of the disordered CH_2Cl_2 and one of the CH_2Cl_2 orientations between the (**ClIO**)$_4$ with distances (Å) and highlighting the unusual solvent imide synthon.

Overall, while solvent molecules are usually viewed as a nuisance in crystal structures and refinement (due to potential disorder and occupancy issues and treated accordingly)[9a], the impact of recent developments in halogen bonding[1,11] puts in perspective how halogenated solvent molecules are crucial in crystal formation, occupying voids in the lattice and contributing to structural stability by a combination of halogen and hydrogen bonding interactions[1-2,11,12] (schemes 2,3). The influence of halogenated solvents (typically chlorinated) is seen to impact and assist in trezimide and tennimide crystal formation and not just to occupy and fill potential voids as solvent filler in the crystal lattice. These results highlight the importance of considering the role that solvents play in assembling and maintaining crystal structures through viable though modest interactions in the absence of strong classical hydrogen bond donors.[10,11]

Isostructural behaviour in the* (MIO)$_4$ *crystal structures

For comparisons with their F, Cl, Br[18c] analogues, two methylated (**MIO**)$_4$ tennimides (crystallising with CH_2Cl_2 and $CHCl_3$, respectively) are reported. They are isostructural and essentially isomorphous with the Cl and Br analogues in space group *Pccn* and differ only in the subtlety of their solvent...O=C(macrocycle) interactions.[10,18]

The CH_2Cl_2 interacts with the two imide carbonyl O atoms from two neighbouring (**MIO**)$_4$ macrocycles. With two C-Cl...O=C halogen bonding interactions forming (N_c = 0.93, 0.96) and CH_2Cl_2 residing on a 2-fold axis, the averaged structure is a disordered CH_2Cl_2 linking the imide-based macrocycles *via* C=O...$ClCH_2Cl$...O=C as O1...$ClCH_2Cl$...O2, but not as O1...X...O1 or O2...X...O2 (where X = CH_2Cl_2). While the halogen bonding distances suggest a modest interaction, the cumulative effect of a favourable C-H...$N_{pyridine}$ plus the two C-Cl...O=C halogen bonds is important in crystal structure formation (Scheme 2; Fig. 6).[1-2,11-12] The CH_2Cl_2 demonstrates a clear role in structure assembly and overall stability.

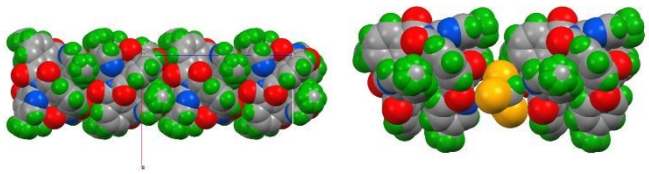

Fig. 6: Views of the $(\mathbf{MIO})_4$ 1D structure along the *b*-axis direction and disordered chloroform interacting with two macrocycles *via* hydrogen and halogen bonding.

The $(\mathbf{MIO})_4\bullet CHCl_3$ structure is similar with the $CHCl_3$ molecules linking macrocycles using two Cl atoms in halogen bonding with the imide O=C, and the chloroform C-H in hydrogen bonding interactions with disordered pyridine N atoms. However, the binding is not as effective as for the CH_2Cl_2 (N_c = 0.96, 0.98) and the $CHCl_3$ molecule exhibits the cyclic $R^2_2(8)$ pattern as noted previously for $(\mathbf{BrIO})_4\bullet CHCl_3$[5c] and $(\mathbf{ClIO})_4\bullet CH_2Cl_2$ (present work). Obviously the role that solvent plays (especially when disordered) in crystal structure formation needs further examination.

While the focus is on the trezimide/tennimide macrocyclic structures as presented, the crystal structures with various solvent molecules facilitate the analysis of unusual solvent:macrocycle synthons and aggregates. The evidence confirms that chlorinated hydrocarbon solvents support crystal formation and with linking of molecules by hydrogen bonding/halogen bonding interactions in trezimide/tennimides into chains, whereas more polar and aprotic solvents are more involved in solvent channel formation. Of further note is the isostructural series of CH_3, Cl and Br tennimides crystallising in space group *Pccn*.[18]

Macrocyclic flexibility and stability

Based on our research and previous reports[5] it can be stated in general terms that the stability and flexibility of tennimides and trezimides depend on two main factors: (*i*) the number of segments or repeat units within the macrocycle (three or four) and (*ii*) the nature of the *para*-substituent on the pyridinyl or pyrimidinyl ring. NMR experimental observations at different temperatures and solvents clearly suggest that, in general, trezimides are more flexible, but less stable than tennimides. As such tennimides are more rigid and stable than trezimides and less prone to hydrolysis in mild acidic conditions or in polar solvents. These conclusions can be drawn from preparative TLC purifications on silica plates as well as from NMR experiments in different solvents. Tennimide stability arises from the favoured conformation of the imide linker [$(O{=}C)_2NR$] that is almost ideal for tetramer cyclisation, without the requirement for significant conformational change (distortion). This imide linker has a preferred conformational twist of ~90°±15° due to steric requirements as seen structurally in all tennimides[5,6] as sequential 'CO···CO' dihedral angles twist within the macrocycles. In contrast the dihedral angles of the trezimides differ remarkably and there is considerable steric strain in some linkers and rings which may be a major reason for the relative instability of trezimides.

Experiences with different tennimides and trezimides suggests that the nature of the substituent at the *para*-position influences the stability of both macrocyclic imides.[5] For example the $(\mathbf{EsIO})_3$ trezimide[5b] can be regarded as 'edge-case' as it was noted to be labile in strong polar solvents such as DMSO, while most other macrocycles are stable, including $(\mathbf{EsIO})_4$. Furthermore, attempts to synthesise tennimides and trezimides bearing a *para*-cyano (–C≡N) group using 6-amino-3-pyridinecarbonitrile failed, even after several trials. Possible explanations may be rationalised in the relationship between the substituent electron-withdrawing/donating properties and imide backbone stability. The macrocyclic imide stability declines with a substituent having stronger electron-withdrawing properties; $(\mathbf{MIO})_4$, $(\mathbf{IO})_{3/4}$, $(\mathbf{26IO})_{3/4}$, $(\mathbf{FIO})_{3/4}$, $(\mathbf{ClIO})_{3/4}$, and $(\mathbf{BrIO})_{3/4}$ are stable,[5] whereas the $(\mathbf{EsIO})_{3/4}$ pair are less stable; therefore, $(\mathbf{CNIO})_{3/4}$ macrocyclic synthesis was not realised by us. One possible explanation is that strong electron density depletion (as expected with **C≡N**, $\mathbf{NO_2}$ and $\mathbf{COOH(CH_3)}$) destabilises the imide bridge. Nevertheless, future synthesis with functional groups such as OH, NH_2, CH_3O, CH_3CH_2, NO_2 *etc*. is required to examine this hypothesis to establish a general rule for overall trezimide and tennimide macrocycle stability.

Conclusions

The four fluorinated and two chlorinated macrocyclic imide crystal structures provide valuable insights into the effects of halogens and solvents in synthon formation, aggregation and supramolecular structures. All eight structures (including the methylated tennimides) are analysed to highlight differences between halogenated solvents and more polar, aprotic solvents such as DMSO. The ^{19}F NMR data indicate the possibility of a second distinct tennimide conformation and there are on-going strategies to try to isolate this and other possible tennimide conformations.

A series of methyl/chloro/bromo tennimides $(\mathbf{XIO})_4$ display isomorphous/isostructural behaviour and with a notable consistent packing in space group *Pccn*.[18] Differences arise only in the fine detail of local halogen/hydrogen bonding and involve the solvent (hydrochlorocarbon) molecules with imide carbonyl and pyridine nitrogen atoms and in macrocycle:solvent aggregate formation. Studies are on-going to examine the 1D/2D/3D aggregation in the crystal structures of these and related macrocycles and the effect of solvent molecules in assisting crystal structure formation and stability. Additional interests are the comprehensive and on-going studies to truly understand atom…atom interactions and how they facilitate aggregation in solution towards crystallisation in the solid-state. The deconvolution of the contribution of important synthons and especially where disorder and or dynamic processes (involving solvents) are present is key to understanding aggregation and the fundamentals of crystal engineering.

Acknowledgements

This research was funded under the Programme for Research in Third Level Institutions (PRTLI) Cycle 4 (Ireland) and was co-funded through the European Regional Development Fund (ERDF), part of the European Union Structural Funds Programme (ESF) 2007–2013.

Notes and references

† Full crystallographic, refinement and structural details for all trezimides and tennimides are provided in the ESI (Section 5.1) together with interaction data.

1 P. Metrangolo and G. Resnati, (Eds.) *Halogen Bonding: Fundamentals and Applications*; Structure and Bonding, **2008,** *126*, Springer, Berlin.
2 (*a*) K. Raatikainen and K. Rissanen, *Chem. Sci*. **2012,** *3*, 1235–1239; (*b*) R. W. Troff, T. Mäkelä, F. Topić, A. Valkonen, K. Raatikainen and K. Rissanen, *Eur. J. Org. Chem*. **2013,** 1617–1637; (*c*) A. Priimagi, G. Cavallo, P. Metrangolo and G. Resnati, *Acc. Chem. Res*. **2013,** *46,* 2686–2695; (*d*) O. Makhothkina, J. Lieffrig, O. Jeannin, M. Fourmigué, E. Aubert and E. Espinosa, *Cryst. Growth Des*. **2015,** *15,* 3464–3473; (*e*) P. S. Ho, *Top. Curr. Chem*. **2015,** *358,* 241–276.
3 (*a*) J. W. Steed and J. L. Atwood, *Supramolecular Chemistry*, **2009,** John Wiley & Sons, West Sussex, 2nd edn.; (*b*) J. W. Steed and P. A. Gale, *Supramolecular Chemistry: from Molecules to Nanomaterials,* Wiley, Hoboken, New Jersey, USA, **2012**, vol. 1–8.
4 (*a*) L. He, Y. An, L. Yuan, W. Feng, M. Li, D. Zhang, K. Yamato, C. Zheng, X. C. Zeng and B. Gong, *Proc. Nat. Acad. Sci. U.S.A.* **2006,** *103,* 10850–10855; (*b*) A. Isidro-Llobet, T. Murillo, P. Bello, A. Cilibrizzi, J. T. Hodgkinson, W. R. J. D. Galloway, A. Bender, M. Welch and D. R. Spring, *Proc. Nat. Acad. Sci. U.S.A.* **2011,** *108,* 6793–6798; (*c*) S. Guieu, A. K. Crane and M. J. MacLachlan, *Chem. Commun*. **2011,** *47,* 1169–1171; (*d*) N. Fujimoto, M. Matsumura, I. Azumaya, S. Nishiyama, H. Masu, H. Kagechika and A. Tanatani, *Chem. Commun*. **2012,** *48*, 4809–4811; (*e*) D. S. Maxwell, D. Sun, Z.-H. Peng, D. V. Martin, B. A. Bhanu Prasad, W. G. Bornmann, *Tet. Lett*. **2013,** *54,* 5799–5801; (*f*) M. F. Geer, J. Mazzuca, M. D. Smith and L. S. Shimizu, *CrystEngComm,* **2013,** *15,* 9923–9929; (*g*) V. Havel, V. Sindelar, M. Necas and A. E. Kaifer, *Chem. Commun*. **2014,** *50,* 1372–1374; (*h*) M. Yamada, R. Kanazawa and F. Hamada, *CrystEngComm*, **2014,** *16,* 2605–2614.
5 (*a*) P. Mocilac and J. F. Gallagher, *J. Org. Chem.* **2013***, 78*, 2355–2361; (*b*) P. Mocilac and J.F. Gallagher, *Acta Crystallogr.* **2013***, B69*, 62–69; (*c*) P. Mocilac and J.F. Gallagher, *CrystEngComm,* **2014***, 16*, 1893–1903.
6 L. S. Evans and P. A. Gale, *Chem. Commun*. **2004,** 1286–1287.
7 Oxford Diffraction Ltd. ABSFAC and CrysAlisPro CCD/RED, *Version 1.171.33.55*, Oxford Diffraction, Abingdon, Oxfordshire, U.K.
8 (*a*) G. M. Sheldrick, *Acta Crystallogr. Sect. A* **2008***, A64*, 112–122; (*b*) P. McArdle, *J. Appl. Cryst.* **1995***, 28*, 65–65.
9 (*a*) A. L. Spek, *J. Appl. Cryst.* **2003***, 36*, 7–13; (*b*) C. F. Macrae, I. J. Bruno, J. A. Chisholm, P. R. Edgington, P. McCabe, E. Pidcock, L. Rodriguez-Monge, R. Taylor, J. van de Streek and P. A. Wood, *J. Appl. Cryst*. **2008**, *41*, 466–470.
10 F. H. Allen, *Acta Crystallogr.* **2002,** *B58,* 380–388.
11 D. S. Yufit and J. A. K. Howard, *CrystEngComm*. **2010,** *12,* 737–741.
12 G. R. Desiraju, P. S. Ho, L. Kloo, A. C. Legon, R. Marquardt, P. Metrangolo, P. Politzer, G. Resnati and K. Rissanen, *Pure and Applied Chemistry*, **2013,** *85,* 1711–1713.
13 K. Durka, S. Luliński, K. N. Jarembska, J. Smętek, J. Serwatowski and K. Woźniak, *Acta Crystallogr. Section B, Structural Science*, **2014,** *B70,* 157–171.
14 S. L. Price, A. J. Stone, J. Lucas, R. S. Rowland and A. E. Thornley, *J. Am. Chem. Soc*. **1994,** *116*, 4910–4918.
15 S. Sengupta, A. Goswami, S. Ganguly, S. Bala, M. K. Bhunia and R. Mondal, *CrystEngComm*. **2011,** *13*, 6136–6149.
16 (*a*) T. T. T. Bui, S. Dahaoui, C. Lecomte, G. R. Desiraju and E. Espinosa, *Angew. Chem*. **2009,** *48,* 3838–3841. (*b*) M. V. Vener, A. V. Shishkina, A. A. Rykounov and V. G. Tsirelson, *J. Phys. Chem*., **2013**, *117*, 8459–8467.
17 (*a*) J. D. Dunitz, *IUCrJ*, **2015**, *2*, 157–158; (*b*) T. S. Thakur, R. Dubey and G. R. Desiraju, *IUCrJ*, **2015,** *2,* 159–160; (*c*) C. Lecomte, E. Espinosa and C. F. Matta, *IUCrJ*, **2015,** *2,* 161–163.
18 (*a*) C. Capacci-Daniel, S. Dehghan, V. M. Wurster, J. A. Basile, R. Hiremath, A. A. Sarjeant and J. A. Swift, *CrystEngComm*. **2008,** *10*, 1875–1880; (*b*) I. D. H. Oswald and W. D. Crichton, *CrystEngComm*. **2008,** *11*, 463–469; (*c*) L. R. Gomes, J. N. Low, F. Cagide and F. Borges, *Acta Crystallogr*. **2015,** *E71*, 88–93.

Table 2: Comparisons of the $(FIO)_3$ and $(ClIO)_3$ trezimides with $(IO)_3$[a] and $(BrIO)_3$[d]

Trezimide (Å)	$(IO)_3$[a]	$(FIO)_3$[b]	$(FIO)_3$[c]	$(ClIO)_3$[c]	$(BrIO)_3$[d]
X...X	3.61 (H...H)	4.059(2)	3.641(2)	3.660(3)	4.4321(13), 4.0315(11)
(**X** = H†, F, Cl, Br)	10.74	10.000(2)	12.006(2)	11.925(3)	10.664(5), 12.765(3)
	12.06	11.463(2)	13.335(3)	13.340(3)	11.555(5), 14.165(3)
H...H(intraannular)	2.67	2.56	2.58	2.57	2.57, 2.53
	2.83	2.76	2.69	2.71	2.80, 2.96
	2.87	2.98	2.84	2.81	2.93, 2.97
N...N$_{tertiary}$	5.117(3)	5.2036(19)	5.1647(19)	5.126(5)	5.168(6), 5.186(6)
N1/N2/N3 atoms	5.280(3)	5.3024(18)	5.3325(18)	5.284(4)	5.342(5), 5.193(6)
	5.311(3)	5.3069(18)	5.4235(19)	5.339(5)	5.434(6), 5.425(6)
N...N$_{pyridine}$	5.033(4)	5.646(2)	5.240(2)	5.266(6)	5.824(7), 5.287(7)
	7.457(3)	6.563(2)	7.917(2)	7.616(5)	6.664(6), 8.102(7)*
	8.843(3)	6.746(2)	9.220(2)	8.926(6)	6.779(7), 9.094(7)*
O...O$_{isophthaloyl}$	6.924(2)	6.6558(17)	6.7660(18)	6.792(5)	6.648(6), 6.723(5)
	6.928(3)	6.908(2)	6.8191(18)	6.853(5)	6.743(6), 6.816(6)
	6.998(3)	7.0351(18)	6.922(2)	6.968(6)	6.995(5), 6.963(6)
O...O$_{imide}$	3.600(2)	3.7358(19)	3.768(2)	3.626(5)	3.459(6), 3.653(6)
	3.656(3)	3.4932(19)	3.807(2)	3.837(5)	3.784(6), 3.708(6)
	3.857(3)	3.8107(18)	3.900(2)	3.896(5)	3.934(7), 3.847(5)

Table 3: $(XIO)_4$ geometric data (Å) (with X = H, F, Cl, CH_3, Br)

Tennimide	**$(IO)_4$** [a]	**$(FIO)_4$** [b]	**$(FIO)_4$** [c]	**$(ClIO)_4$** [d]	**$(MIO)_4$** [e]	**$(BrIO)_4$** [f]
Cavity	*oc*	*oc*	*cc*	*Oc*	*oc*	*oc*
X...X	9.27 $_{H...H}$ 9.58 9.90 10.29 10.64 10.90	9.804(4) 9.901(4) 10.254(4) 10.647(5) 10.778(5) 10.978(4)	10.091(4) 10.230(5) 10.336(4) 10.355(5) 10.373(5) 10.566(4)	10.7944(15) 10.9513(11) 11.0232(11) 11.359(2)	10.429(9) 10.65(3) 10.88(3) 11.65(5)	11.0808(9) 11.1123(8) 11.3021(8) 11.8026(15)
$H...H_{intra}$	3.00, 3.00 3.20, 3.23 4.13, 4.33	3.00, 3.08 3.08, 3.13 4.11, 4.31,	3.12, 3.13 3.22, 3.24 4.34, 4.35	3.04, 3.16 4.10, 4.37	3.06, 3.19 4.15, 4.37	3.02, 3.19 4.13, 4.35
$N...N_{tertiary}$	5.196(3) - 5.360(3); 5.729(3) 5.976(3)	5.162(4) 5.312(4) 5.358(4) 5.381(4) 5.645(4) 5.816(4)	5.238(3) 5.246(3) 5.252(3) 5.307(3) 5.824(3) 5.939(3)	5.195(3) 5.346(3) 5.696(4) 5.867(5)	5.198(4) 5.342(4) 5.755(5) 5.909(5)	5.198(4) 5.358(4) 5.685(7) 5.935(6)
$H...N_{pyridine}$	2.85, 3.92	2.80, 3.31	3.01, 3.08	2.91, 3.43	2.93, 3.48	2.64, 2.96
$O...O_{isophthaloyl}$	6.670(3) - 6.967(3)	6.631(3) 6.664(4) 6.753(4) 6.989(3)	6.840(3) 6.850(4) 6.867(3) 6.918(3)	6.843(3) 6.844(2)	6.852(4) 6.869(4)	6.869(4) 7.050(4)
$O...O_{imide}$	3.485(3) - 3.758(3)	3.398(4) 3.635(4) 3.753(4) 3.763(4)	3.543(4) 3.548(4) 3.548(4) 3.551(3)	3.506(3) 3.633(3)	3.507(4) 3.629(4)	3.524(5) 3.652(5)

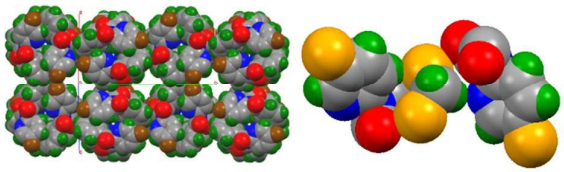

The role of halogenated and aprotic solvents in macrocyclic structures is assessed in terms of halogen and hydrogen bonding interactions.